

Location-Aided Coordinated Analog Precoding for Uplink Multi-User Millimeter Wave Systems

Flavio Maschietti[‡], David Gesbert[‡], Paul de Kerret[‡]

[‡]Communication Systems Department, EURECOM, Sophia-Antipolis, France

Email: {flavio.maschietti, david.gesbert, paul.dekerret}@eurecom.fr

Abstract

Millimeter wave (mmWave) communication is expected to have an important role in next generation cellular networks, aiming to cope with the bandwidth shortage affecting conventional wireless carriers. Using side-information has been proposed as a potential approach to accelerate beam selection in mmWave massive MIMO (m-MIMO) communications. However, in practice, such information is not error-free, leading to performance degradation. In the multi-user case, a wrong beam choice might result in irreducible inter-user interference at the base station (BS) side. In this paper, we consider location-aided precoder design in a mmWave uplink scenario with multiple users (UEs). Assuming the existence of direct device-to-device (D2D) links, we propose a decentralized coordination mechanism for robust fast beam selection. The algorithm allows for improved treatment of interference at the BS side and in turn leads to greater spectral efficiencies.

I. INTRODUCTION

The large bandwidths available at mmWave carrier frequencies are expected to help meet the throughput requirements for future mobile networks [1]. Since smaller wavelength signals are more prone to absorption, mmWave communications require beamforming in order to guarantee appropriate link margins and coverage [2], [3]. To this end, m-MIMO techniques [4] are envisioned as high-gain directional antennas with small form factor can be designed for mmWave usage [5]. However, configuring those massive antennas to operate with large bandwidths entails an additional effort. The high cost and power consumption of the radio components impact on the UEs and small BSs, thus limiting the practical implementation of a fully-digital beamforming architecture [1]. Moreover, the large number of antennas at both ends of the radio links would require unfeasible CSI-training overhead to design the precoders.

One step towards simplification consists in replacing the fully-digital architecture with a *hybrid* analog-digital one [6]–[11]. In mixed analog-digital architectures, a low-dimensional digital processor is concatenated with an RF analog beamformer, implemented through phase shifters. Note that while the latter is sufficient to achieve a good part of the overall beamforming gain – through beam steering towards desired spatial directions – the digital stage is essential when processing multiple streams and users.

Interestingly, existing works on hybrid architectures typically ignore multi-user interference issues in the analog domain and cope with them in the digital part. For instance, in [12], a procedure is proposed for the downlink transmission, where the analog stage is intended to find the best beam directions for each UE (regardless of multi-user interference), while the digital one applies the conventional Zero-Forcing (ZF) beamformer on the resulting effective channel. The strength of this approach lies in the fact that it is possible to use the existing beam training algorithms for single-user links – such as [13]–[15] – in the analog stage. Such algorithms have been developed bearing in mind the need for fast link establishment in low-latency applications. Nevertheless, the reduced number of digital chains might not always allow to resolve the residual multi-user interference which remains after the analog beamforming stage. In particular, in a mmWave propagation scenario [2], [3], multiple closely located UEs will likely share some common reflectors, causing an alignment of the main path’s angles of arrival at the BS receiver and preventing it from resolving the interference, even at the digital decoding stage.

To solve this problem, a principal idea consists in treating interference before it takes place, i.e. the UE side, as is done for example in [16], [17]. Although showing significant performance advantages over the existing solutions, these works assume perfect CSIR for analog beamforming and single-antenna UEs, which might not be realistic in all mmWave contexts [12].

Rather, we are interested in statistically-driven analog beamforming at the UE TX side. In this paper, we point out that simple analog UE beam selection can be designed so as to enable the analog receive beam on the BS side to discriminate for interference. We propose to do this through the help of low-rate side-information at the UEs. Several works can be found in the mmWave literature, where side-information is exploited to improve performance without burdening overhead. Side-information can be obtained from various sources, such as automotive sensors [18], UHF band [19], GNSS [20], or also past multipath fingerprints measurements [21].

We bring forward the idea that position-based side-information can be exploited in order to develop a coordination mechanism between the UEs, so that the interference at the BS side can

be treated efficiently through both the analog and digital parts of the receiver, as opposed to relying on the digital part alone. The main intuition is to use coordination to make sure the selected analog beams at the BS convey the full rank of multi-user channels towards the digital part to preserve invertibility.

As in some previous work [22], we are interested in establishing a *robust* form of coordination which accounts for possible noise in the positioning information made available to the UEs. However, [22] targets a single-user scenario only. In the multi-user scenario, the lack of a real-time communication channel prevents the UEs from exchanging instantaneous CSI. We consider, instead, the existence of a low-rate unidirectional D2D channel, allowing communication of GPS-type data. In particular, we consider a hierarchical set-up where higher ranked UEs receive position information from lower ranked ones. The unidirectional aspect and the limitation to position information exchange help keep the D2D overhead much lower than real-time D2D. Our main contributions read as follows:

- We formulate the problem of per-user analog precoding with side position information and recast it as a *decentralized* beam selection problem.
- Our algorithm exploits the hierarchical structure of the information, in order to perform robust (with respect to position data noise) interference mitigation at both analog and digital stages.
- Under the proposed method, the UEs coordinate to select beams which, while being sub-optimal in terms of average power, help attain the full rank condition needed at the BS for interference suppression.

II. SYSTEM MODEL

Consider the single-cell uplink multi-user mmWave scenario in Fig. 1. The BS is equipped with $N_{\text{BS}} \gg 1$ antennas to support K UEs with $N_{\text{UE}} \gg 1$ antennas each. The UEs are assumed to reside in a disk of a given radius r_{cl} , which will be used to control inter-UE average distance. Each UE sends one data stream to the BS. We assume that the BS has $N_{\text{RF}} = K$ RF chains available, each one connected to all the N_{BS} antennas, assuming a fully-connected hybrid architecture [1].

The u -th UE precodes the data $s^u \in \mathbb{C}$ through the analog precoding vector $\mathbf{v}^u \in \mathbb{C}^{N_{\text{UE}} \times 1}$. We assume that the UEs have one RF chain each, i.e. UEs are limited to analog beamforming via phase shifters (constant-magnitude elements) [7]. In addition, $\mathbb{E}[\|\mathbf{v}^u s^u\|^2] \leq 1$, assuming normalized power constraints.

The reconstructed signal after mixed analog/digital combining at the BS can be expressed as follows – assuming no timing and carrier mismatches:

$$\hat{\mathbf{x}} = \sum_{u=1}^K \mathbf{W}_D \mathbf{W}_{\text{RF}}^H \mathbf{H}^u \mathbf{v}^u s^u + \mathbf{W}_D \mathbf{W}_{\text{RF}}^H \mathbf{n} \quad (1)$$

where $\mathbf{H}^u \in \mathbb{C}^{N_{\text{BS}} \times N_{\text{UE}}}$ is the channel matrix from the u -th UE to the BS and $\mathbf{n} \in \mathbb{C}^{N_{\text{BS}} \times 1}$ is the thermal noise vector, with zero mean and covariance matrix $\sigma_{\mathbf{n}}^2 \mathbf{I}_{N_{\text{BS}}}$. $\mathbf{W}_{\text{RF}} \in \mathbb{C}^{N_{\text{BS}} \times N_{\text{RF}}}$ is, instead, the analog combining matrix, containing the vectors relative to each of the K RF chains (subject to the same hardware constraints as described above), while $\mathbf{W}_D \in \mathbb{C}^{K \times N_{\text{RF}}}$ denotes the digital combining matrix.

The received SINR for the u -th UE at the BS is expressed as follows:

$$\gamma^u = \frac{|\mathbf{w}_D^u \mathbf{W}_{\text{RF}}^H \mathbf{H}^u \mathbf{v}^u|^2}{\sum_{w \neq u} |\mathbf{w}_D^u \mathbf{W}_{\text{RF}}^H \mathbf{H}^w \mathbf{v}^w|^2 + \sigma_{\tilde{\mathbf{n}}}^2} \quad (2)$$

where $\mathbf{w}_D^u \in \mathbb{C}^{1 \times N_{\text{RF}}}$ denotes the row of \mathbf{W}_D related to the u -th UE (one RF chain for each UE), and where we used the short-hand notation $\tilde{\mathbf{n}} = \mathbf{W}_D \mathbf{W}_{\text{RF}}^H \mathbf{n}$ for the filtered thermal noise.

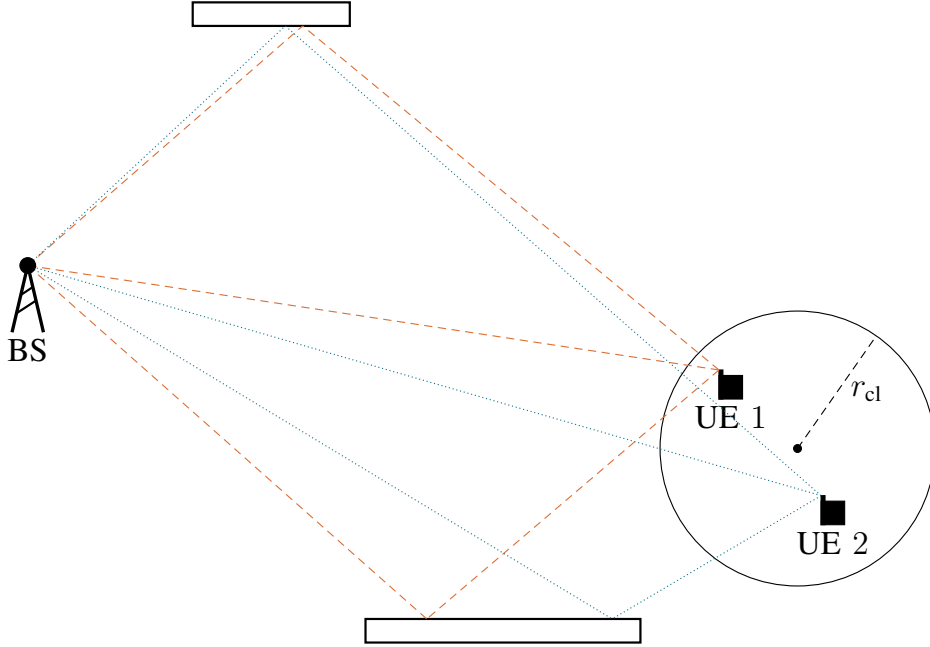


Fig. 1: Scenario example with $L = 3$ propagation paths, two reflectors, and $K = 2$ UEs. The UEs are assumed to reside in a disk of radius r_{cl} , which is relatively common in realistic scenarios, e.g. dense UE distribution in a coffee house. In this illustration, two closely located UEs are sharing some reflectors, and paths reflecting on the top reflector arrive quasi-aligned at the BS while originating from distinct UEs.

A. Channel Model

Unlike the conventional UHF band propagation environment, the mmWave one does not exhibit rich-scattering [2] and is in fact modeled as a geometric channel with a limited number of dominant propagation paths which survive high attenuation. The UE u is thus subject to the channel matrix $\mathbf{H}^u \in \mathbb{C}^{N_{\text{BS}} \times N_{\text{UE}}}$, expressed as the sum of L components or contributions [7]:

$$\mathbf{H}^u = (N_{\text{BS}}N_{\text{UE}})^{1/2} \left(\sum_{\ell=1}^L \alpha_{\ell}^u \mathbf{a}_{\text{BS}}(\vartheta_{\ell}^u) \mathbf{a}_{\text{UE}}^{\text{H}}(\phi_{\ell}^u) \right) \quad (3)$$

where $\alpha_{\ell}^u \sim \mathcal{CN}(0, (\sigma_{\ell}^u)^2)$ denotes the complex gain for the ℓ -th path of the u -th UE. Furthermore, we assume that the variances $(\sigma_{\ell}^u)^2, \ell \in \{1, \dots, L\}; u \in \{1, \dots, K\}$ of the paths are such as $\sum_{\ell} (\sigma_{\ell}^u)^2 = 1, \forall u \in \{1, \dots, K\}$.

The variables $\phi_{\ell}^u \in [0, 2\pi)$ and $\vartheta_{\ell}^u \in [0, 2\pi)$ are the angles of departure (AoDs) and arrival (AoAs) for each contribution, for a given UE u , where one angle pair corresponds to the LoS direction while other might account for the presence of strong reflectors (e.g. buildings, hills) in the environment. The positions of those points of reflection depend on the position of the considered UE (see Fig. 1). We will denote the reflecting points for the u -th UE with $\mathbf{R}_i^u, i \in \{1, \dots, L-1\}$ in the rest of the paper.

The vectors $\mathbf{a}_{\text{UE}}(\phi_{\ell}^u) \in \mathbb{C}^{N_{\text{UE}} \times 1}$ and $\mathbf{a}_{\text{BS}}(\vartheta_{\ell}^u) \in \mathbb{C}^{N_{\text{BS}} \times 1}$ denote the antenna steering vectors at the u -th UE and the BS for the corresponding AoDs ϕ_{ℓ}^u and AoAs ϑ_{ℓ}^u , respectively.

We assume to use ULAs at both sides, so that [23]:

$$\mathbf{a}_{\text{UE}}(\phi) = \frac{1}{(N_{\text{UE}})^{1/2}} \left[1, e^{-i\pi \cos(\phi)}, \dots, e^{-i\pi(N_{\text{UE}}-1) \cos(\phi)} \right]^{\text{T}} \quad (4)$$

$$\mathbf{a}_{\text{BS}}(\vartheta) = \frac{1}{(N_{\text{BS}})^{1/2}} \left[1, e^{-i\pi \cos(\vartheta)}, \dots, e^{-i\pi(N_{\text{BS}}-1) \cos(\vartheta)} \right]^{\text{T}} \quad (5)$$

B. Codebooks for Analog Beams

The most recognized method to implement the analog beamformer is through a network of *digitally-controlled* phase shifters [24] (refer to [1] for alternative architectures). Thus, the phase of each element of the analog beamformer is limited to fixed quantized values, and therefore, the beamforming vectors need to be selected from a finite set (or codebook). We denote the codebooks used for analog beamforming as:

$$\mathcal{V}_{\text{UE}} = \{\mathbf{v}_1, \dots, \mathbf{v}_{M_{\text{UE}}}\}, \quad \mathcal{V}_{\text{BS}} = \{\mathbf{w}_1, \dots, \mathbf{w}_{M_{\text{BS}}}\} \quad (6)$$

where \mathcal{V}_{UE} is assumed to be shared between all the UEs, to ease the notation.

For ULAs, a suitable design for the fixed beamforming vectors in the codebook consists in selecting steering vectors over a discrete grid of angles [12], [14]:

$$\mathbf{v}_p = \mathbf{a}_{\text{UE}}(\bar{\phi}_p), \quad p \in \{1, \dots, M_{\text{UE}}\} \quad (7)$$

$$\mathbf{w}_q = \mathbf{a}_{\text{BS}}(\bar{\vartheta}_q), \quad q \in \{1, \dots, M_{\text{BS}}\} \quad (8)$$

where the angles $\bar{\phi}_p, \forall p \in \{1, \dots, M_{\text{UE}}\}$ and $\bar{\vartheta}_q, \forall q \in \{1, \dots, M_{\text{BS}}\}$ can be chosen according to different strategies, including regular and non-regular sampling of the $[0, \pi]$ range [22].

Remark 1. Given the one-to-one correspondence between the beamforming vectors in \mathcal{V}_{BS} (resp. \mathcal{V}_{UE}), and the grid angles $\bar{\vartheta}_q, \forall q \in \{1, \dots, M_{\text{BS}}\}$ (resp. $\bar{\phi}_p, \forall p \in \{1, \dots, M_{\text{UE}}\}$), we will make the abuse of notation $q \in \mathcal{V}_{\text{BS}}$ (resp. $p \in \mathcal{V}_{\text{UE}}$) to denote the vector $\mathbf{w}_q \in \mathcal{V}_{\text{BS}}$ (resp. $\mathbf{v}_p \in \mathcal{V}_{\text{UE}}$). \square

III. INFORMATION MODEL

In this section, we describe the structure of the channel state- and side-information available at both UEs and BS sides. We start with defining the nature of information in an ideal setting before turning to a realistic (*noisy*) case.

Definition 1. *The average beam gain matrix $\mathbf{G}^u \in \mathbb{R}^{M_{\text{BS}} \times M_{\text{UE}}}$ contains the power level associated with each combined choice of analog beam pair between the BS and the u -th UE after averaging over small scale fading. It is defined as:*

$$G_{q,p}^u = \mathbb{E}_{\boldsymbol{\alpha}^u} \left[|\mathbf{w}_q^H \mathbf{H}^u \mathbf{v}_p|^2 \right] \quad (9)$$

where the expectation is carried out over the channel coefficients $\boldsymbol{\alpha}^u = [\alpha_1^u, \alpha_2^u, \dots, \alpha_L^u]$ and with $G_{q,p}^u$ denoting the (q, p) -element of \mathbf{G}^u .

Definition 2. *The position matrix $\mathbf{P}^u \in \mathbb{R}^{2 \times (L+1)}$ contains the two-dimensional location coordinates $\mathbf{p}_n^u = [p_{n_x}^u \quad p_{n_y}^u]^T$ for node n , where n indifferently refers to either the BS, the u -th UE or one of the reflectors $\mathbf{R}_i^u, i \in \{1, \dots, L-1\}$. It is defined as follows:*

$$\mathbf{P}^u = \begin{bmatrix} \mathbf{p}_{\text{BS}}^u & \mathbf{p}_{\text{R}_1}^u & \cdots & \mathbf{p}_{\text{R}_{L-1}}^u & \mathbf{p}_{\text{UE}}^u \end{bmatrix} \quad (10)$$

We will denote as \mathcal{P} the set containing all the position matrices $\mathbf{P}^u, \forall u \in \{1, \dots, K\}$.

As shown in [22], the matrix \mathbf{G}^u can be expressed as a function of the matrix \mathbf{P}^u . We recall here the deterministic relationship that is found between those two matrices.

Lemma 1. *We can write the average beam gain matrix relative to the u -th UE as follows:*

$$G_{q,p}^u(\mathbf{P}^u) = \sum_{\ell=1}^L (\sigma_\ell^u)^2 |L_{\text{BS}}(\Delta_{\ell,q}^u)|^2 |L_{\text{UE}}(\Delta_{\ell,p}^u)|^2 \quad (11)$$

where we remind the reader that $(\sigma_\ell^u)^2$ denotes the variance of the channel coefficients α_ℓ^u and we have defined:

$$L_{\text{UE}}(\Delta_{\ell,p}^u) = \frac{1}{(N_{\text{UE}})^{1/2}} \frac{e^{i(\pi/2)\Delta_{\ell,p}^u}}{e^{i(\pi/2)N_{\text{UE}}\Delta_{\ell,p}^u}} \frac{\sin((\pi/2)N_{\text{UE}}\Delta_{\ell,p}^u)}{\sin((\pi/2)\Delta_{\ell,p}^u)} \quad (12)$$

$$L_{\text{BS}}(\Delta_{\ell,q}^u) = \frac{1}{(N_{\text{BS}})^{1/2}} \frac{e^{i(\pi/2)\Delta_{\ell,q}^u}}{e^{i(\pi/2)N_{\text{BS}}\Delta_{\ell,q}^u}} \frac{\sin((\pi/2)N_{\text{BS}}\Delta_{\ell,q}^u)}{\sin((\pi/2)\Delta_{\ell,q}^u)} \quad (13)$$

and

$$\Delta_{\ell,p}^u = (\cos(\bar{\phi}_p) - \cos(\phi_\ell^u)) \quad (14)$$

$$\Delta_{\ell,q}^u = (\cos(\vartheta_\ell^u) - \cos(\bar{\vartheta}_q)) \quad (15)$$

with the angles $\phi_\ell^u, \ell \in \{1, \dots, L\}$ and $\vartheta_\ell^u, \ell \in \{1, \dots, L\}$ obtained from the position matrix \mathbf{P}^u through simple algebra (refer to [22] for more details).

A. Distributed Noisy Information Model

In the distributed model, each UE u receives its own estimates of the position matrices $\mathbf{P}^w, \forall w \in \{1, \dots, K\}$. We will use the superscript with parenthesis (u) to denote any information known at the u -th UE. In particular, we denote as $\hat{\mathbf{P}}^{w,(u)} \in \mathbb{R}^{2 \times (L+1)}, \forall w \in \{1, \dots, K\}$ the local information available at the u -th UE about the position matrix \mathbf{P}^w . This information is modeled as follows:

$$\hat{\mathbf{P}}^{w,(u)} = \mathbf{P}^w + \mathbf{E}^{w,(u)} \quad \forall w \in \{1, \dots, K\} \quad (16)$$

where $\mathbf{E}^{w,(u)}$ denotes the following matrix:

$$\mathbf{E}^{w,(u)} = \begin{bmatrix} \mathbf{e}_{\text{BS}}^{w,(u)} & \mathbf{e}_{\text{R}_1}^{w,(u)} & \dots & \mathbf{e}_{\text{R}_{L-1}}^{w,(u)} & \mathbf{e}_{\text{UE}}^{w,(u)} \end{bmatrix} \quad (17)$$

containing the random position errors which the u -th UE made in estimating \mathbf{p}_n^w . Such error comes with an arbitrary, yet known, probability density function $f_{\mathbf{e}_n^{w,(u)}}$.

Definition 3. *We will denote as $\hat{\mathcal{P}}^{(u)}$, where:*

$$\hat{\mathcal{P}}^{(u)} = \{\hat{\mathbf{P}}^{1,(u)}, \dots, \hat{\mathbf{P}}^{K,(u)}\} \quad (18)$$

the overall local information available at the u -th UE containing all the estimated position matrices $\hat{\mathbf{P}}^{w,(u)}, \forall w \in \{1, \dots, K\}$.

B. Hierarchical Location-Information Exchange

The hierarchical (or nested) model is a sub-case of the distributed model in which the u -th UE has access to the estimates of the UEs $u + 1, \dots, K$. As we will see in the next section, this information structure enables some coordination for just half of the overhead needed in a conventional two-way exchange mechanism. One consequence in particular is that the u -th UE is able to retrieve the beam decisions carried out at (the less informed) UEs $u + 1, \dots, K$.

C. Additional Information

In what follows the number of dominant paths, and their average powers $(\sigma_\ell^u)^2, \ell \in \{1, \dots, L\}; u \in \{1, \dots, K\}$ are assumed to be known at each UE, based on prior averaged measurements. Likewise, statistical distributions $f_{e_n^{w,(u)}}, \forall u, w$ are supposed to be quasi-static and as such are supposed to be available to each UE. In other words, the u -th UE is aware of the amount of error in the position estimates which it and other UEs have to cope with.

IV. MULTI-USER LOCATION-AIDED HYBRID PRECODING

In order to maximize the received SNR γ^u defined in (2) for each UE, the mutual optimization of both analog and digital components must be taken into account. A common approach consists in decoupling the design, as the analog beamformer can be optimized in terms of long-term channel statistics, whereas the digital one can be made dependent on instantaneous information [25].

A. Uncoordinated Beam Selection

We first review here the approach given in [12], where the authors proposed to design the analog beamformers to maximize the received power for each UE, neglecting multi-user interference. Once the analog beamformers are fixed at both UE and BS sides, the design of the digital beamformer at the BS follows the conventional MU-MIMO approach. In this respect, a common choice is to consider ZF combining. Therefore, the digital beamforming matrix \mathbf{W}_D is the pseudo-inverse of the effective channel matrix $\tilde{\mathbf{H}} \in \mathbb{C}^{N_{\text{RF}} \times K}$, which is defined as follows [23]:

$$\mathbf{W}_D = (\tilde{\mathbf{H}}^H \tilde{\mathbf{H}})^{-1} \tilde{\mathbf{H}}^H \quad (19)$$

where

$$\tilde{\mathbf{H}} = \left[\mathbf{W}_{\text{RF}}^H \mathbf{H}^1 \mathbf{v}^1 \quad \mathbf{W}_{\text{RF}}^H \mathbf{H}^2 \mathbf{v}^2 \quad \dots \quad \mathbf{W}_{\text{RF}}^H \mathbf{H}^K \mathbf{v}^K \right], \text{ and with } \mathbf{W}_{\text{RF}} = \left[\mathbf{w}^1 \quad \mathbf{w}^2 \quad \dots \quad \mathbf{w}^K \right].$$

When position and path average power information is available, the beam selection ($q_u^{\text{un}} \in \mathcal{V}_{\text{BS}}, p_u^{\text{un}} \in \mathcal{V}_{\text{UE}}$) at the analog stage of the algorithm proposed in [12] – which we will denote as *uncoordinated* (un) – can be expressed as follows:

$$(q_u^{\text{un}}, p_u^{\text{un}}) = \underset{\substack{q_u \in \mathcal{V}_{\text{BS}} \\ p_u \in \mathcal{V}_{\text{UE}}}}{\text{argmax}} \mathcal{R}^u(\hat{\mathcal{P}}^{(u)}, q_u, p_u), \quad \forall u \quad (20)$$

where we have defined the single-user rate \mathcal{R}^u as [22]:

$$\mathcal{R}^u(\mathcal{P}, q_u, p_u) = \log_2 \left(1 + \frac{G_{q_u, p_u}^u(\mathbf{P}^u)}{\sigma_{\mathbf{n}}^2} \right) \quad (21)$$

Equation (20) can be solved through direct search of the maximum in the matrix \mathbf{G}^u , derived from $\hat{\mathcal{P}}^{(u)}$ through (11).

While being simple to implement, the information at each UE in this method is treated as perfect, although some Bayesian robustization can be introduced [22]. Another limitation of this approach is that each UE solves its own beam selection problem in a way which is independent of other UEs, thus ignoring the possible impairments in terms of interference. We illustrate this effect in Fig. 2, where we plot the mean rate per UE obtained when the analog precoders are chosen through (20), in case of $K = 2$ UEs, *perfect* position information, as a function of r_{cl} . As the inter-UE average distance decreases, the performance of this procedure degrades, since the UEs have much more chance to share common best propagation paths (which results in severe interference at the analog stage at the BS). The action of the ZF is noticeable but not sufficient for small cluster radii. In what follows, we consider different flavors of coordination.

B. Naive-Coordinated Beam Selection

In order to improve performance, we design the analog precoders according to the following figure of merit, which takes into account the average multi-user interference at the analog stage:

$$\mathcal{R}(\mathcal{P}, q_{1:K}, p_{1:K}) = \sum_{u=1}^K \log_2 \left(1 + \frac{G_{q_u, p_u}^u(\mathbf{P}^u)}{\sum_w G_{q_u, p_w}^w(\mathbf{P}^w) + \sigma_{\mathbf{n}}^2} \right) \quad (22)$$

Remark 2. We used here the short-hand $q_{1:K}, p_{1:K}$ to denote the indexes q_1, \dots, q_K and p_1, \dots, p_K , respectively. \square

The hierarchical model allows the u -th UE to predict the beam selected at UEs $u + 1, \dots, K$. However, for a full coordination, the u -th UE would also need to know the precoding strategies of the *more* informed UEs, i.e. UE $1, \dots, u - 1$, which involves some guessing [26].

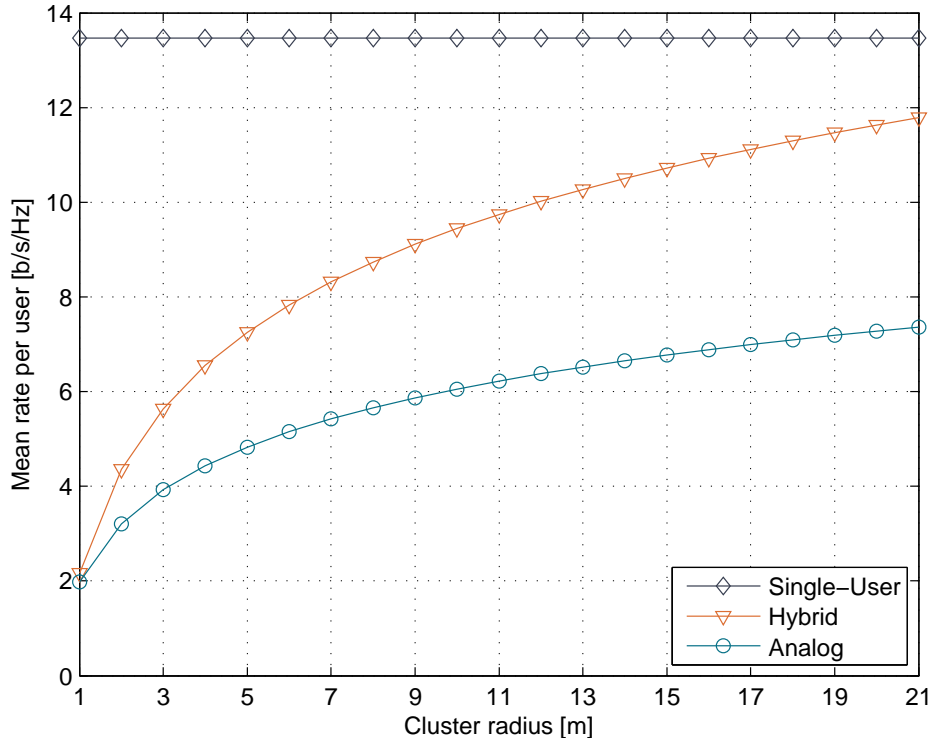


Fig. 2: Mean rate per UE vs Cluster radius. The performance degrades *sharply* as the inter-UE average distance decreases.

As a first approximation, the u -th UE can assume that its estimates are *perfect* (error-free) and *global* (shared between all the UEs). Since UEs $1, \dots, u-1$ have in fact different estimates, and since such information is not error-free, we call this approach *naive-coordinated* (nc). The beam indexes ($q_u^{\text{nc}} \in \mathcal{V}_{\text{BS}}, p_u^{\text{nc}} \in \mathcal{V}_{\text{UE}}$) associated to the u -th UE are then found as follows:

$$(\tilde{q}_{1:u-1}, q_u^{\text{nc}}, \tilde{p}_{1:u-1}, p_u^{\text{nc}}) = \underset{\substack{q_1, \dots, q_u \in \mathcal{V}_{\text{BS}} \\ p_1, \dots, p_u \in \mathcal{V}_{\text{UE}}}}{\text{argmax}} \mathcal{R}_{q_{u+1:K}, p_{u+1:K}} \left(\hat{\mathcal{P}}^{(u)}, q_{1:u}, p_{1:u} \right) \quad (23)$$

Remark 3. We make here an abuse of notation. The subscripts $q_{u+1:K}, p_{u+1:K}$ acknowledge for the known strategies at the u -th UE. Those strategies are fixed parameters of the function \mathcal{R} . The same notation will be used in the rest of the paper. \square

Remark 4. The u -th UE will use the precoding vector associated to the index $p_u^{\text{nc}} \in \mathcal{V}_{\text{UE}}$ to reach the BS and will discard the remaining beam indexes $\tilde{q}_{1:u-1}, \tilde{p}_{1:u-1}$ found for the other UEs. Indeed, those indexes only correspond to guesses realized at the u -th UE which do not necessarily correspond to the true beams used for transmission at UEs $1, \dots, u-1$. We have introduced the notation \tilde{q}_u to denote such beams. \square

C. Statistically-Coordinated Beam Selection

The naive-coordinated approach relies on the correctness of the position estimates available at each UE. As a consequence, its performance is expected to degrade in case of GPS inaccuracies or lost location awareness. As the precision of position estimates decreases, the beam selection is expected to have more confidence in long-term statistics alone, to predict the behavior of the UE which are higher ranked in the information chain. In this case, the position estimates are not exploited, and each UE relies on prior statistics to figure out other UEs' information. We denote the resulting *statistically-coordinated* (sc) beam indexes relative to the u -th UE as $(q_u^{\text{sc}} \in \mathcal{V}_{\text{BS}}, p_u^{\text{sc}} \in \mathcal{V}_{\text{UE}})$, which read as follows:

$$(\tilde{q}_{1:u-1}, q_u^{\text{sc}}, \tilde{p}_{1:u-1}, p_u^{\text{sc}}) = \underset{\substack{q_1, \dots, q_u \in \mathcal{V}_{\text{BS}} \\ p_1, \dots, p_u \in \mathcal{V}_{\text{UE}}}}{\text{argmax}} \mathbb{E}_{\mathcal{P}|r_{\text{cl}}} \left[\mathcal{R}_{q_{u+1:K}, p_{u+1:K}}^o \left(\mathcal{P}, q_{1:u}, p_{1:u} \right) \right] \quad (24)$$

This is a long-term optimization which is updated only if prior statistics change. Thus, (24) represents a simple stochastic optimization problem [27] which can be solved through e.g. approximation of the expectation operator (carried out over prior statistics) with Monte-Carlo iterations.

D. Robust-Coordinated Beam Selection

The UEs have also access to the statistics of their local position estimates. In the previous approach, each UE used prior statistics to guess the precoding strategies of the more informed UEs. This helps in case the local information available at the u -th UE is not accurate enough to gain more knowledge about the UEs $1, \dots, u-1$. In the opposite case, local statistical information can be exploited to supplement prior information. In this approach, the UEs look for beam selection strategies which *progressively* pass from exploiting local information only – in case of perfect local information – to exploiting statistical information only – in case of poor local information. We denote this approach as *robust-coordinated* (rc). The beams $(q_u^{\text{rc}} \in \mathcal{V}_{\text{BS}}, p_u^{\text{rc}} \in \mathcal{V}_{\text{UE}})$ for the u -th UE are obtained through:

$$(\tilde{q}_{1:u-1}, q_u^{\text{rc}}, \tilde{p}_{1:u-1}, p_u^{\text{rc}}) = \underset{\substack{q_1, \dots, q_u \in \mathcal{V}_{\text{BS}} \\ p_1, \dots, p_u \in \mathcal{V}_{\text{UE}}}}{\text{argmax}} \mathbb{E}_{\mathcal{P}|\hat{\mathcal{P}}^{(u)}, r_{\text{cl}}} \left[\mathcal{R}_{q_{u+1:K}, p_{u+1:K}}^o \left(\mathcal{P}, q_{1:u}, p_{1:u} \right) \right] \quad (25)$$

Remark 5. Here, the u -th UE considers its locally-available position estimates as *imperfect* and *globally*-shared. \square

Also in this case, an approximate solution can be obtained through Monte-Carlo methods, generating possible matrices \mathcal{P} according to the (known) distribution $\mathcal{P}|\hat{\mathcal{P}}^{(u)}, r_{\text{cl}}$.

We summarize the proposed robust-coordinated beam selection used at the u -th UE in Algorithm 1. In Step 1, the u -th UE retrieves the processing carried out at less informed UEs $u + 1, \dots, K$. The K -th UE skips this step. In Step 2, beam selection is performed through (22) (an approximation) and (25).

Algorithm 1 $f_{\text{rc}} : \text{Robust-Coordinated Beam Selection (} u\text{-th UE)}$

INPUT: $\hat{\mathcal{P}}^{(w)}, \forall w \in \{u, \dots, K\}$, pdf of $(\mathcal{P}|\hat{\mathcal{P}}^{(w)}, r_{\text{cl}}), \forall w \in \{u, \dots, K\}$

Step 1

- 1: **for** $w = K : u + 1$ **do** ▷ The K -th UE skips this decreasing *for* loop
- 2: $(q_w^o, p_w^o) = f_{\text{rc}}(\hat{\mathcal{P}}^{(w)}, q_{w+1:K}^o, p_{w+1:K}^o)$

3: **end for**

Step 2

- 4: **return** $(q_u^{\text{rc}}, p_u^{\text{rc}}) \leftarrow \text{Evaluate (25)}$ ▷ Refer to Algorithm 2 for implementation details
-

Algorithm 2 Implementation details for Step 2 in Algorithm 1 (u -th UE)

INPUT: $\hat{\mathcal{P}}^{(u)}$, pdf of $(\mathcal{P}|\hat{\mathcal{P}}^{(u)}, r_{\text{cl}}), q_{u+1}^o, \dots, q_K^o, p_{u+1}^o, \dots, p_K^o$

- 1: **for** $i = 1 : M$ **do** ▷ Approximate expectation over $(\mathcal{P}|\hat{\mathcal{P}}^{(u)}, r_{\text{cl}}), \forall w$ with M Monte-Carlo iterations
 - 2: Generate possible position matrices \mathcal{P} through sampling over the distribution $(\mathcal{P}|\hat{\mathcal{P}}^{(u)}, r_{\text{cl}})$
 - 3: Compute possible gain matrices $\hat{\mathbf{G}}^w, \forall w \in \{1, \dots, K\}$ through (11) using the generated \mathcal{P}
 - 4: SUMRATEEVAL($\hat{\mathbf{G}}^1, \dots, \hat{\mathbf{G}}^K, q_{u+1}^o, \dots, q_K^o, p_{u+1}^o, \dots, p_K^o$) ▷ Described in Algorithm 3
 - 5: **end for**
 - 6: Compute the average sum-rate over the Monte-Carlo iterations for all possible beam pairs
 - 7: $(q_u^{\text{rc}}, p_u^{\text{rc}}) \leftarrow$ Indexes relative to the beams achieving maximum average sum-rate
 - 8: The pair of vectors with indexes $(q_u^{\text{rc}}, p_u^{\text{rc}})$ is assigned to the u -th UE
-

V. SIMULATION RESULTS

We evaluate here the performance of the proposed algorithms. We consider $L = 3$ multipath components. A distance of 100 m is assumed from the UEs' cluster center and the BS. The radius of the UEs' cluster is set to $r_{\text{cl}} = 7$ m. Both the BS and UEs are equipped with $N_{\text{UE}} = N_{\text{BS}} = 64$ antennas (ULA). The number of elements in the beam codebooks is $M_{\text{UE}} = M_{\text{BS}} = 64$, with grid angles spaced according to the inverse cosine function so as to guarantee equal gain losses among adjacent angles [22]. All the plotted rates are the averaged – over 10000 Monte-Carlo runs – rates per UE.

Algorithm 3 Function evaluating an approximated average sum-rate (22) (u -th UE)

```

1: function SUMRATEEVAL( $\hat{\mathbf{G}}^1, \dots, \hat{\mathbf{G}}^K, q_{u+1}^o, \dots, q_K^o, p_{u+1}^o, \dots, p_K^o$ )
2:   KnownInds =  $\{q_{u+1}^o, \dots, q_K^o, p_{u+1}^o, \dots, p_K^o\}$ 
3:   for  $w = 1 : u - 1$  do ▷ The most informed UE 1 skips this loop
4:      $(q_w, \dots, q_u, p_w, \dots, p_u) = \max(\hat{G}_{q_w, p_w}^w / (\sum_{v \neq w} \hat{G}_{q_w, p_w}^v + N_0))$  ▷ with given KnownInds
5:     KnownInds =  $\{q_w, p_w\} \cup \text{KnownInds}$  ▷ Updated set of indexes to be used in the next iteration
6:     Discard all the other indexes  $q_{w+1}, \dots, q_u, p_{w+1}, \dots, p_u$ 
7:   end for
8:   return  $(\hat{G}_{q_u, p_u}^u / (\sum_{w \neq u} \hat{G}_{q_u, p_u}^w + N_0))$  for all possible  $q_u, p_u$  ▷ with given KnownInds
9: end function

```

A. Location Information Model

In the simulations, we adopt a uniform bounded error model for location information [20], [22]. In particular, we assume that all the position estimates lie somewhere inside disks centered in the actual positions $\mathbf{p}_n^u, n \in \{\text{UE}, \text{BS}, \mathbf{R}_i^u\}; i \in \{1, \dots, L - 1\}; u \in \{1, \dots, K\}$. Let $S(r)$ be the two-dimensional closed ball centered at the origin and of radius r , which is $S(r) = \{\mathbf{v} \in \mathbb{R}^2 : \|\mathbf{v}\| \leq r\}$. We model the estimation errors $\mathbf{e}_n^{w,(u)}$ as a random variable *uniformly* distributed in $S(r_n^{w,(u)})$, where $r_n^{w,(u)}$ is the maximum positioning error for the node n of the w -th UE as seen from the u -th UE.

B. Results and Discussion

To evaluate the performance, we start with a simple configuration with $K = 2$ UEs.

1) *Strong LoS*: In what follows, we consider a stronger (on average) LoS path with respect to the reflected paths, being indeed the prominent propagation driver in mmWave bands [2], [3]. The reflected paths are assumed to have the same average power. The average power of such paths is assumed to be shared across the UEs, i.e. $(\sigma_\ell^{(1)})^2 = (\sigma_\ell^{(2)})^2, \forall \ell \in \{1, \dots, L\}$.

In Fig. 3, we consider the performance of the proposed algorithm as a function of the precision of the information available at the less informed UE. In particular, an error radius of 5 m means $r_n^{w,(2)} = 5$ m, $\forall w, n$. As for the most informed UE, we consider *perfect* information in Fig. 3a, i.e. $r_n^{w,(1)} = 0$ m, $\forall w, n$, and 3 m of precision in Fig. 3b, i.e. $r_n^{w,(1)} = 3$ m, $\forall w, n$.

Fig. 3a and Fig. 3b show that both the uncoordinated and the naive approaches degrade fast as the error radius for the less informed UE increases. This is due to the fact that the UEs build their

strategies according to their available position estimates, which become unreliable to perform beam selection. In particular, when the precision is less than 6 m, the statistically-coordinated approach – based on statistical information only – behaves better. The robust-coordinated approach outperforms all the other algorithms, being able to discriminate for interference at the BS side, while taking into account the noise present in position information.

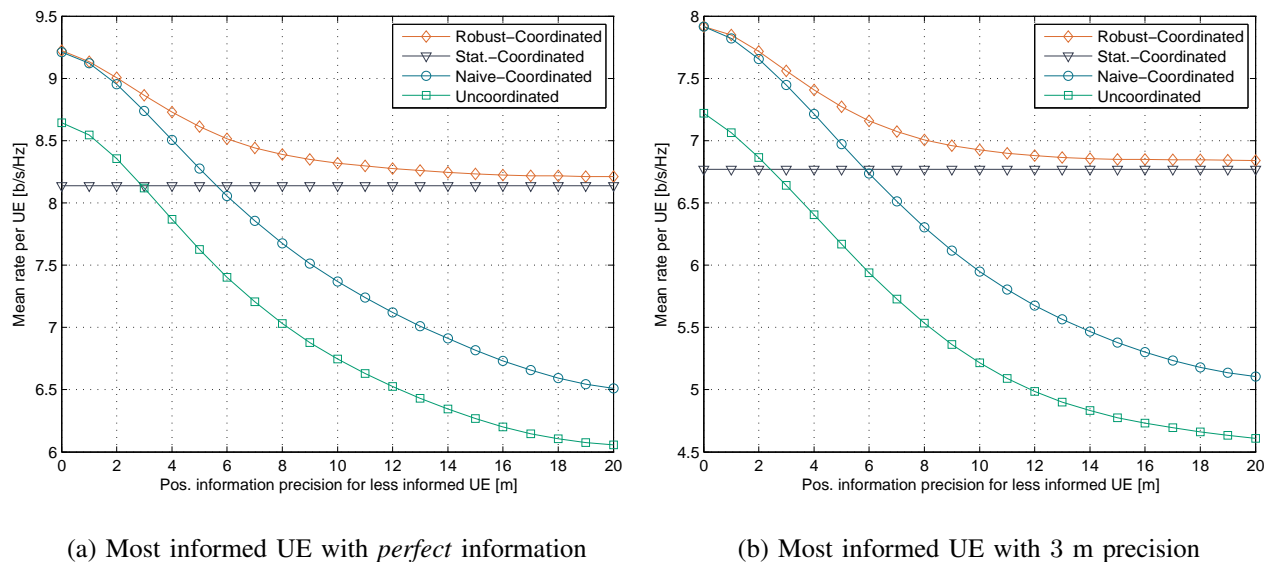


Fig. 3: Mean rate per UE vs Position information precision. Strong LoS.

2) *LoS Blockage*: It is also interesting to observe how the proposed algorithms behave in case of total line-of-sight blockage, while having one stronger reflected path.

Fig. 4 compares the proposed algorithms as a function of the error radius for the less informed UE. The most informed UE is assumed to have access to *perfect* information. The same considerations outlined for the strong LoS case remain valid. It is possible to observe that the uncoordinated approach performs worse than before (with strong LoS), since the UEs choose to use the beams pointing towards the same stronger reflected path. As a consequence, there is much more chance to arrive at the BS with non-distinguishable AoAs. In such cases, coordination between the UEs is essential to combat multi-user interference.

VI. CONCLUSIONS

In mmWave communications, multi-user interference has to be handled in the analog stage as well. In this respect, suitable strategies for multi-user interference minimization can be applied in the beam domain through e.g. exploitation of location-dependent information.

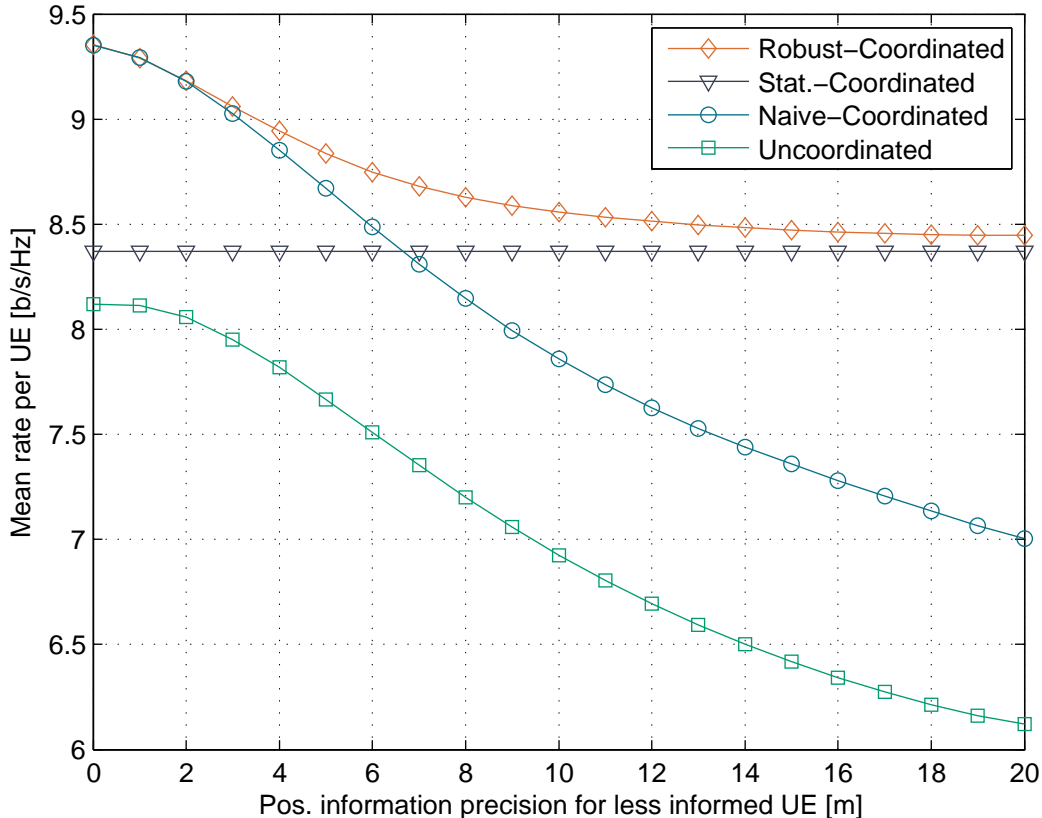


Fig. 4: Mean rate per UE vs Position information precision. LoS blockage.

Dealing with the imperfections in location information is not trivial, due to the decentralized nature of the information, which leads to disagreements between the UEs affecting performance. In this work, we introduced a decentralized robust algorithm which aim to select the best precoder for each UE taking both the noise present in location information and multi-user interference in the analog stage into account.

Numerical experiments have shown that good performance can be achieved with the proposed algorithm and have confirmed that coordination is essential to counteract inter-UE interference in mmWave multi-user environments.

Exploiting Machine Learning tools [28] for solving the proposed algorithms in a more efficient manner is an interesting and challenging problem which we aim to tackle in future studies.

ACKNOWLEDGMENTS

F. Maschietti, D. Gesbert and P. de Kerret are supported by the ERC under the European Union's Horizon 2020 research and innovation program (Agreement no. 670896).

REFERENCES

- [1] R. W. Heath, N. González-Prelcic, S. Rangan, W. Roh, and A. M. Sayeed, "An overview of signal processing techniques for millimeter wave MIMO systems," *IEEE J. Sel. Topics Signal Process.*, Apr. 2016.
- [2] M. R. Akdeniz, Y. Liu, M. K. Samimi, S. Sun, S. Rangan, T. S. Rappaport, and E. Erkip, "Millimeter wave channel modeling and cellular capacity evaluation," *IEEE J. Sel. Areas Commun.*, June 2014.
- [3] T. S. Rappaport, G. R. MacCartney, M. K. Samimi, and S. Sun, "Wideband millimeter-wave propagation measurements and channel models for future wireless communication system design," *IEEE Trans. Commun.*, Sept. 2015.
- [4] L. Lu, G. Y. Li, A. L. Swindlehurst, A. Ashikhmin, and R. Zhang, "An overview of massive MIMO: Benefits and challenges," *IEEE J. Sel. Topics Signal Process.*, Oct. 2014.
- [5] B. Biglarbegian, M. Fakharzadeh, D. Busuioc, M. R. Nezhad-Ahmadi, and S. Safavi-Naeini, "Optimized microstrip antenna arrays for emerging millimeter-wave wireless applications," *IEEE Trans. Antennas Propag.*, May 2011.
- [6] O. E. Ayach, S. Rajagopal, S. Abu-Surra, Z. Pi, and R. W. Heath, "Spatially sparse precoding in millimeter wave MIMO systems," *IEEE Trans. Wireless Commun.*, Mar. 2014.
- [7] A. Alkhateeb, O. E. Ayach, G. Leus, and R. W. Heath, "Channel estimation and hybrid precoding for millimeter wave cellular systems," *IEEE J. Sel. Topics Signal Process.*, Oct. 2014.
- [8] F. Sohrabi and W. Yu, "Hybrid digital and analog beamforming design for large-scale antenna arrays," *IEEE J. Sel. Topics Signal Process.*, Apr. 2016.
- [9] C. Rusu, R. Mèndez-Rial, N. González-Prelcic, and R. W. Heath, "Low complexity hybrid precoding strategies for millimeter wave communication systems," *IEEE Trans. Wireless Commun.*, Dec. 2016.
- [10] K. Venugopal, A. Alkhateeb, N. González-Prelcic, and R. W. Heath, "Channel estimation for hybrid architecture-based wideband millimeter wave systems," *IEEE J. Sel. Areas Commun.*, Sept. 2017.
- [11] F. Sohrabi and W. Yu, "Hybrid analog and digital beamforming for mmWave OFDM large-scale antenna arrays," *IEEE J. Sel. Areas Commun.*, Jul. 2017.
- [12] A. Alkhateeb, G. Leus, and R. W. Heath, "Limited feedback hybrid precoding for multi-user millimeter wave systems," *IEEE Trans. Wireless Commun.*, Nov. 2015.
- [13] J. Wang, "Beam codebook based beamforming protocol for multi-Gbps millimeter-wave WPAN systems," *IEEE J. Sel. Areas Commun.*, Oct. 2009.
- [14] S. Hur, T. Kim, D. J. Love, J. V. Krogmeier, T. A. Thomas, and A. Ghosh, "Millimeter wave beamforming for wireless backhaul and access in small cell networks," *IEEE Trans. Commun.*, Oct. 2013.
- [15] D. Ogbe, D. J. Love, and V. Raghavan, "Noisy beam alignment techniques for reciprocal MIMO channels," *IEEE Trans. Signal Process.*, Oct. 2017.
- [16] J. Li, L. Xiao, X. Xu, and S. Zhou, "Robust and low complexity hybrid beamforming for uplink multiuser mmWave MIMO systems," *IEEE Commun. Lett.*, June 2016.
- [17] Y. Zhu and T. Yang, "Low complexity hybrid beamforming for uplink multiuser mmWave MIMO systems," in *Proc. IEEE Wireless Commun. and Netw. Conf. (WCNC)*, Mar. 2017.
- [18] J. Choi, V. Va, N. González-Prelcic, R. Daniels, C. R. Bhat, and R. W. Heath, "Millimeter-wave vehicular communication to support massive automotive sensing," *IEEE Commun. Mag.*, Dec. 2016.
- [19] A. Ali, N. González-Prelcic, and R. W. Heath, "Millimeter wave beam-selection using out-of-band spatial information," *CoRR*, Feb. 2017. [Online]. Available: <http://arxiv.org/abs/1702.08574>
- [20] N. Garcia, H. Wymeersch, E. G. Ström, and D. Slock, "Location-aided mm-wave channel estimation for vehicular communication," in *Proc. IEEE Int. Workshop on Signal Process. Advances in Wireless Commun. (SPAWC)*, Jul. 2016.

- [21] V. Va, J. Choi, T. Shimizu, G. Bansal, and R. W. H. Jr., "Inverse multipath fingerprinting for millimeter wave V2I beam alignment," *CoRR*, 2017. [Online]. Available: <http://arxiv.org/abs/1705.05942>
- [22] F. Maschietti, D. Gesbert, P. de Kerret, and H. Wymeersch, "Robust location-aided beam alignment in millimeter wave massive MIMO," *Proc. IEEE Global Telecommun. Conf. (GLOBECOM)*, Dec. 2017.
- [23] D. Tse and P. Viswanath, *Fundamentals of Wireless Communication*. Cambridge University Press, 2005.
- [24] Y. Yu, *et al.*, "A 60 GHz phase shifter integrated with LNA and PA in 65 nm CMOS for phased array systems," *IEEE J. Solid-State Circuits*, Sept. 2010.
- [25] Z. Li, S. Han, and A. F. Molisch, "Optimizing channel-statistics-based analog beamforming for millimeter-wave multi-user massive MIMO downlink," *IEEE Trans. Wireless Commun.*, Jul. 2017.
- [26] Y.-C. Ho and K.-C. Chu, "Team decision theory and information structures in optimal control problems," *IEEE Trans. Autom. Control*, Feb. 1972.
- [27] A. Shapiro, D. Dentcheva, and A. Ruszczyński, *Lectures on stochastic programming: modeling and theory*. Philadelphia, PA, USA: Society for Industrial and Applied Mathematics, 2014.
- [28] C. Rasmussen and C. Williams, *Gaussian Processes for Machine Learning*, ser. Adaptive Computation and Machine Learning. Cambridge, MA, USA: The MIT Press, 2006.